

Transcutaneous Dual Tuned RF Coil System Voltage Gain and Efficiency Evaluation for a Passive Implantable Atrial Defibrillator

Omar J Escalona¹, Jose J Velasquez², Niall Waterman¹, Lawrence Chirwa¹, John Anderson¹

¹University of Ulster, Newtownabbey, Northern Ireland

²Universidad Simón Bolívar, Caracas, Venezuela

Abstract

Cardioversion of atrial fibrillation (AF) can be achieved by applying an electric shock to the heart (defibrillation). A cost-effective approach for internal cardioversion is by means of a subcutaneous passive implantable atrial defibrillator (PIAD). A circuit design using a dual tuned resonant circuit whose capacitance on the receiver side also serves as a voltage booster is proposed and evaluated. The circuit performance is characterised using a MATLAB based model and a PSpice simulation. The circuit exhibited inherent voltage gain stability with a reasonable voltage gain ($V_{Rx} / V_{Tx} > 0.3$). Computed link efficiency modelling, estimated high link efficiency values of about 63.63% at the 208 kHz resonant frequency (26 mm air gap between coils). The above theoretical characterisation was supported by hardware prototyping which realised a system efficiency of 59.61% (best case).

1. Introduction

Medical investigations have found that AF is the most common sustained cardiac arrhythmia which can occur in the presence or absence of structural heart disease [1]. Patients suffering from AF will have a significantly increased risk of developing a stroke. In the field of healthcare, several options for the treatment of AF are available including pharmacological cardioversion, electrical cardioversion, pacemaker based therapies and atrial ablation techniques. In the past few years, interest in the field of catheter-based transvenous internal defibrillation has increased [2-4].

Internal atrial defibrillation can be achieved with rectangular monophasic waveforms using voltage levels in the order of 100 V, and energy levels around 0.7 J - 3 J [2]. It is therefore important when designing a portable defibrillator to consider efficiency ways of powering the device and delivering energy to the patient. Another important factor that needs to be taken into consideration

is the shape of the defibrillation waveform. Rectilinear low-tilt pulse waveforms have been shown to have a higher success rate than those of conventional capacitor discharge defibrillation which presents an exponential decay pulse waveform [3].

This paper presents a proposed circuit that, in addition to being energy efficient (approximately 59.61% in the best case), produces stable low-tilt pulses (3.5% in the best result obtained), which is desirable for a portable transdermal defibrillation device.

2. Methods

A transcutaneous wireless instant power transmission system is used to deliver a rectangular pulse internally into the heart. A circuit performance study for a proposed transcutaneous method of atrial defibrillation, by means of radio frequency (RF) coupled coils, is presented. System voltage gain and efficiency evaluation was carried out on several coil prototypes. The coils in these prototypes are separated by a 26 mm air gap to simulate the worst case skin thickness. A basic overview of the system is shown in figure 1.

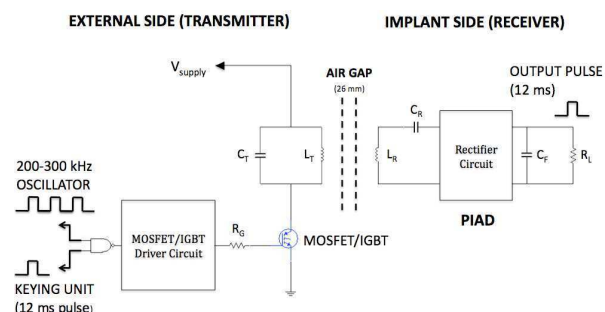


Figure 1. Overview of transmitter/receiver prototype.

The transdermal atrial defibrillator is based on a wireless power coupling system between a RF driven coil on the transmitter side and an implanted coil on the receiver side. The transmitter coil is typically excited for 12 ms (keying pulse) by a RF (200 kHz to 300 kHz)

signal. After the induced magnetic field generates a voltage in the receiver coil, the induced voltage is then rectified and filtered to produce a rectangular shaped output pulse. The output pulse is then delivered to a nominal 50Ω dummy load which simulates the impedance of the heart.

Theoretical analysis of the system shown in figure 1 is complicated by the rectifier circuit in the receiver which presents different secondary topological configurations for the positive and negative waveforms. In order to analyze the link efficiency of the system, a simplified circuit model is adopted. This circuit model includes the parasitic series resistance for the transmitter and receiver but ignores the distributed capacitance in the coils, see figure 2. In theory, maximum power transfer to the load and overall system efficiency will occur at the resonant frequency. At this frequency, the reactive components in the circuit will cancel out and the power will largely be dissipated by the resistive components.

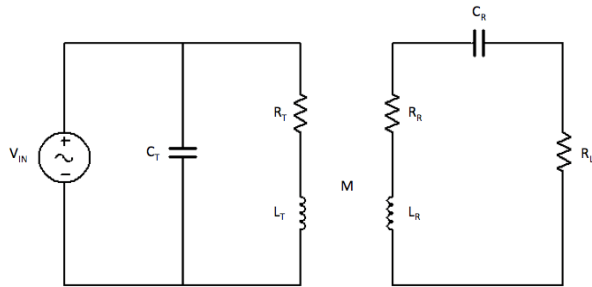


Figure 2. Simplified circuit model of dual tuned system.

The schematic circuit shown in figure 2 depicts the specific case of parallel resonance in the transmitter and series resonance in the receiver. This parallel transmitter-series receiver configuration is characterized as a current in/current out topology [4]. This type of topology provides current magnification in the transmitter (parallel resonance) and voltage magnification in the receiver (series resonance). Using an analytical model for the schematic circuit, the impedance of the receiver (Z_{Rx}) and the transmitter (Z_{Tx}) circuit can be expressed as follows:

$$Z_{Rx} = (R_R + R_L) + j \left(\omega \cdot L_R - \frac{1}{\omega \cdot C_R} \right) \quad (1)$$

$$Z_{Tx} = \frac{R_T + R_{REF} + j \cdot \omega \cdot L_T}{1 + (R_T + R_{REF})j \cdot \omega \cdot C_T - \omega^2 \cdot C_T \cdot L_T} \quad (2)$$

From Figure 2, the reflected impedance Z_{REF} from the receiver to the transmitter circuit can be written as:

$$Z_{REF} = \frac{\omega^2 \cdot M^2 (R_R + R_L)}{(R_R + R_L)^2 + \left(\omega \cdot L_R - \frac{1}{\omega \cdot C_R} \right)^2} + j \left[\frac{\omega^2 \cdot M^2 \left(\omega \cdot L_R - \frac{1}{\omega \cdot C_R} \right)}{(R_R + R_L)^2 + \left(\omega \cdot L_R - \frac{1}{\omega \cdot C_R} \right)^2} \right] \quad (3)$$

Referring to the equations presented in this section, the variables L_T and L_R are the self-inductance values for the transmitter and receiver windings, R_T and R_R are the parasitic series resistance shown in the inductor model for each coil respectively, M is the mutual inductance between the coils, ω represents the angular frequency and R_L is the load resistance. In theory, the reactive components in the receiver circuit will cancel at the resonant frequency (ω_0). From equations (1), (2) and (3), this results in the following:

$$C_R = \frac{1}{\omega_0^2 \cdot L_R} \quad (4)$$

$$C_T = \frac{L_T}{\omega^2 \cdot L_T^2 + (R_T + R_{REF})} \quad (5)$$

In equations 4 and 5, the variables C_R and C_T represent the receiver and transmitter resonance capacitors respectively. The link efficiency (η) is defined as the product between the transmitter (η_T) and receiver (η_R) circuit efficiencies respectively. All the efficiencies can be expressed as follows:

$$\eta_T = \frac{\text{Power delivered to receiver circuit}}{\text{Total power handled by the transmitter circuit}} \quad (6)$$

$$\eta_R = \frac{\text{Power delivered to the load}}{\text{Total power handled by the receiver circuit}} \quad (7)$$

$$\eta = \frac{M^2 \cdot R_L}{(R_R + R_L)[R_T \cdot L_R \cdot C_R (R_R + R_L) + M^2]} \quad (8)$$

The equations resulting from the circuit analysis are derived from an approach proposed by Gaddam [5]. The equations have been modified to our particular RF model and use design parameters obtained from theoretical methods. The skin and proximity effect given by Terman [6] have also been included to simulate the influence of the AC resistance in the circuit. The following factors are used as inputs in the corresponding MATLAB model:

- Transmitter and receiver series resistance
- Transmitter and receiver self-inductance
- Mutual inductance
- Output load resistor
- Skin and proximity effect modelling factors

Table 1 shows the self and mutual inductance values used in the MATLAB modelling of each RF coil. These values were calculated using both Wheeler's [7] and Grover's [8] methods respectively. The geometric form of

the coil was used to approximately calculate its DC series resistance. All the coils used in this study have 30 turns of wire and fixed inner diameter of 20 mm.

Table 1. Self and Mutual Inductance calculated using Wheeler's and Grover's methods (Tx coil diameter = Rx coil diameter).

Wire Diameter (mm)	Wheeler's Self-Inductance (μH)	Grover's Self-Inductance (μH)	Grover's Mutual Inductance (μH)
0.85	39.65152	39.08186	3.52135
0.75	38.32394	38.20410	2.93303
0.40	34.88795	34.42536	1.28710

3. Results

The stability of the output voltage across a 50 ohm intracardiac impedance model was theoretically evaluated by determining its variations as a function of coil separation. Figure 3 reveals that the family of graphs follow a similar "S" shape curve. This means as the coil separation decreases the link efficiency increases (curve shifts to the left) and as the coil separation increases the link efficiency decreases (curve shifts to the right), assuming that the same operating frequency is maintained.

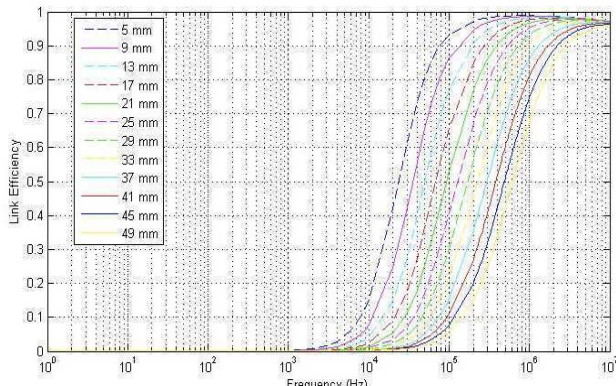


Figure 3. Link efficiency versus operating resonant frequency as a function of coil separation.

As an example, selecting 240 kHz as an operating frequency and a 25 mm separation, the theoretical link efficiency value obtained is 0.7305. If the distance is decreased by a factor of 16%, the link efficiency will increase by a factor of 10.34%. However, if the distance is increased by 16% then the link efficiency will drop by a factor of 13.61%. This demonstrates how sensitive the link efficiency is to coil separation, due to its direct relationship with the mutual inductance between the coils.

Computer modeling estimated a link efficiency value of 63.63% at the 208 kHz resonant frequency for a 26 mm separation between coils. Table 2 presents the values obtained from the developed MATLAB model.

Table 2. Summary of simulation results from MATLAB model.

Resonant Frequency (kHz)	Tx/Rx Wire Diameter (mm)	Rx/Tx Resonant Capacitor (nF)	Link Efficiency	
			Without AC Effects	With AC Effects
208	0.85	17.40/17.41	0.7545	0.6363
211	0.75	14.89/13.57	0.6458	0.5354
212	0.40	16.38/16.38	0.1152	0.0993

For comparison, figure 4 presents the link efficiency (includes the skin and proximity effect model) for the three matching coil diameter prototypes detailed in table 3. The graphs reveal that the three individual plots have a similar "S" shape curve to that shown in figure 3.

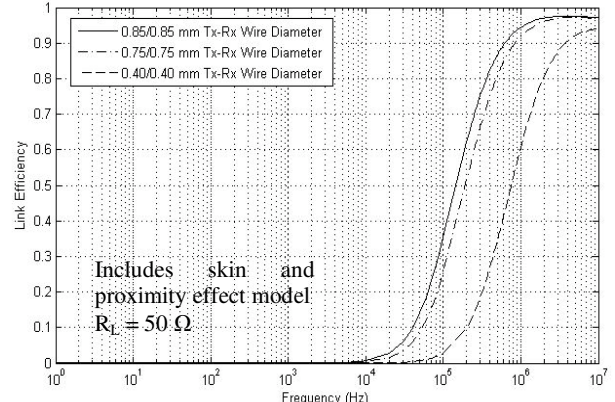


Figure 4. Link efficiency versus operating resonant frequency as a function of coil separation for the three matching coil diameter prototypes.

Figure 5 presents the practical results obtained from the hardware implementation of the system shown in figure 1. The prototype was powered from a supply voltage of approximately 50 V_{DC} and used both a MOSFET and an IGBT as a power switch on the transmitter side. A full-wave voltage doubler with two secondary windings wired in a central tapped configuration was employed on the receiver side. Transformer test with the 0.85 mm wire diameter prototype gave an overall system efficiency of 59.61% (MOSFET, best case). This figure agrees closely with the 63.63% value predicted by the computer model.

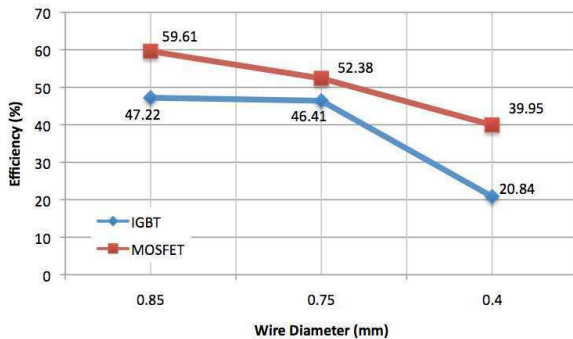


Figure 5. Overall efficiency versus wire diameter for matching coil diameter prototypes ($V_{\text{supply}} \approx 50 \text{ V}_{\text{DC}}$).

Figure 6 presents the results obtained from our PSpice simulation study (circuits tuned for a frequency of 256 kHz). For the specify case of 25 mm separation between coils, we can observe that an overall voltage gain of approximately -9 dB is obtained at 270 kHz. This figure converts to a linear voltage gain of 0.354 ($V_{\text{Rx}}/V_{\text{Tx}}$). This gain figure is similar to the experimental voltage gain measure in an analogous hardware prototype employing a half-wave voltage doubler in the receiver with a 26 mm separation between coils. The prototype was powered from an approximate average voltage of 49 V_{DC} and the measured average output was 14.4 V (MOSFET, $f_o = 270 \text{ kHz}$), i.e. gain of 0.294 ($V_{\text{Rx}}/V_{\text{Tx}}$).

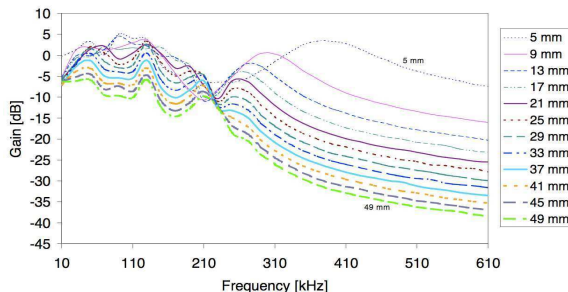


Figure 6. Gain-frequency characteristics for proposed 0.85/0.85 mm Tx-Rx coil diameter circuit with 30 turns.

4. Conclusions and further work

It has been shown that a voltage gain of approximately one-third is achievable with the hardware prototype circuit operating from a 50 V_{DC} supply, characterized with reliable overall system efficiency over 40% (transformer prototypes with 0.75 mm and 0.85 mm). In order to realize a higher voltage level of 100 V in the receiver side, a minimum of 300 V_{DC} will be required on the transmitter side. Current work at the Centre for Advanced Cardiovascular Research (CACR) is involved with the development of a higher voltage prototype that is

powered from a lithium-ion battery and controlled from a microcontroller. The first phase of this development work is expected to be completed early next year.

Acknowledgements

This work was supported by funding from Invest Northern Ireland and the European Regional Development Fund.

References

- [1] Wyndham C. Atrial fibrillation: the most common arrhythmia. Texas Heart Institute J, 2000; 27(3):257-267.
- [2] Walsh SJ, Manoharan G, Escalona OJ, Santos J, Evans N, Anderson JMcC, et al. Novel rectangular biphasic and monophasic waveforms delivered by a radiofrequency-powered defibrillator in transvenous cardioversion of atrial fibrillation. Europeace, 2006; 8:873-880.
- [3] Glover BM, McCann CJ, Manoharan G, Walsh SJ, Moore MJ, Allen JD, et al. A pilot study of a low-tilt biphasic waveform for transvenous cardioversion of atrial fibrillation: improved efficacy compared with conventional capacitor-based waveforms in patients. PACE, 2008; 31:1020-1024.
- [4] Santos JA. Transcutaneous pulsed mode power delivery to implants for treatment of atrial fibrillation. PhD Thesis, University of Ulster, UK; 2002.
- [5] Gaddam V. Remote power delivery for hybrid integrated bio-implantable electrical stimulation system [dissertation]. Baton Rouge (USA): Louisiana State University; 2005.
- [6] Terman F. Radio engineering handbook. 1st ed. New York and London: McGraw-Hill book company; 1943. p. 26-127.
- [7] Wheeler HA. Simple inductance formulas for radio coils. Proceeding of the IRE, 1928; 16(10):1398-1400.
- [8] Grover FW. Inductance calculations: working formulas and Tables. 1st ed. New York: Dover Publications Inc.; 1946. p. 82-113.

Address for correspondence.

Professor Omar J. Escalona
University of Ulster, NIBEC
Centre for Advanced Cardiovascular Research (CARC)
Shore Road, Newtownabbey, Co. Antrim
BT37 0QB
United Kingdom
E-mail: oj.escalona@ulster.ac.uk